8 (3): 229-234 (2024)

Journal of Aviation

https://dergipark.org.tr/en/pub/jav

e-ISSN 2587-1676

Effect of Laser Surface Texturing Process on Dry Sliding Wear Behavior of NiTi Shape Memory Alloy Used in Airplane

Yılmaz Küçük[1*], Emre Altaş[2], M. Sabri Gök[3] and Hüseyin Bahar [4]

[1*]Bartin University, Faculty of Engineering, Architecture and Design, Department of Mechanical Engineering, 74100, Bartın, Türkiye. (ykucuk@bartin.edu.tr)
[2]Bartin University, Faculty of Engineering, Architecture and Design, Department of Mechanical Engineering, 74100, Bartın, Türkiye. (emrealtas@bartin.edu.tr)
[3]Bartin University, Faculty of Engineering, Architecture and Design, Department of Mechanical Engineering, 74100, Bartın, Türkiye. (msabrigok@bartin.edu.tr)
[4] Bartin University, Institute of Science, Department of Mechanical Engineering, 74100, Türkiye Bartın, Türkiye. (aslankartal_00@hotmail.com)

Article Info

Received: 16 September 2024
Revised: 25 September 2024
Accepted: 29 September 2024
Published Online: 06 October 2024

Keywords:
NiTi
Shape memory alloy
Laser Surface Texturing
Dry sliding wear

Corresponding Author: *Yılmaz Küçük*

RESEARCH ARTICLE

https://doi.org/10.30518/jav.1551063

Abstract

In this study, the effect of laser surface texturing (LST) applied to NiTi Shape Memory Alloy (SMA) on the dry sliding wear behavior of the material was investigated. After polishing and cleaning the material surface, a pitted surface texturing process was performed using a femtosecond laser under atmospheric conditions. After the surface texturing process, dry sliding wear tests were performed at room temperature. When the wear behavior of the laser-applied and non-laser-applied test samples was evaluated comparatively, it was determined that the coefficient of friction (COF) of the laser-applied samples under 1N load was approximately 17% lower. It was determined that the decrease in the COF value decreased with increasing load. However, the wear amount of the LSD-applied NiTi SMA was higher than the untreated sample. It was evaluated that this situation was due to thermal softening that occurred depending on the ablation geometry and dimensions.

1. Introduction

Shape memory alloys (SMAs), in their most general expression, are materials that have the property of returning to their original shape or size when heated after deformation in the cold state. It belongs to the class of shape memory materials (SMAs) that have the property of returning to their previous form or shape as a result of mechanical, magnetic, or thermomechanical effects (Jani, Leary, Subic, & Gibson, 2014). One of the reasons for the high ductility of NiTi SMAs is the low elastic anisotropy (Otsuka & Ren, 2005). The shape memory property of these alloys occurs as a result of the shape change or thermoelastic martensite transformation taking place by the twinning mechanism instead of the sliding mechanism. SMAs can exist in two possible phases with three different crystal structures (twinned martensitic, untwinned martensitic, and austenite) and six different transformations (Sun & Huang, 2009). While the austenitic structure is stable at high temperatures, the martensitic structure is stable at low temperatures.

The first use of NiTi SMAs began in 1963, and from 1973 onwards, they were used in biomedical applications such as braces, stents, and implants. After 1980, they became one of the preferred materials in the automotive, space, and aviation fields. In recent years, significant advancements have been made in shape memory alloys, which can change their properties in response to environmental conditions and convert one form of energy into another. The use of smart materials is rapidly increasing in industries such as biomedical, textile, aerospace, and automotive (Fig.1). The literature summary provides a concise and effective overview of key studies focused on improving the tribological properties of materials used in aerospace applications. When the studies are examined, Abedini et al. studied the wear behavior of a Ti-50.3 at% Ni alloy against bearing steel under different loads and sliding distances. It was found that increasing the load from 40 N to 60 N reduced the wear rate due to the formation of iron-rich oxide layers. Similarly, longer sliding distances at higher loads (60 N and 80 N) also decreased wear, attributed to more stable oxide layers forming on the alloy's surface (Abedini, Ghasemi, & Ahmadabadi, 2012). DellaCorte et al. evaluated 60NiTi spherical bearings for aerospace and industrial use, focusing on their tribological performance. The bearings, tested under 4.54 kN loads and exposed to hydraulic and deicing fluids, performed comparably to stainless steel bearings. The results showed 60NiTi as a corrosion-resistant, viable material for these applications (DellaCorte & Jefferson, 2015). Wang et al., the study focuses on enhancing the tribological properties of titanium alloys using laser surface alloying and cladding. In-situ composite coatings like Cr7C3/NiCr, Ti5Si3/Ti, and Ti5Si3/NiTi2 were created on titanium substrates. The research evaluates the coatings'

tribological performance at room and elevated temperatures, analyzing how microstructural features and laser processing conditions affect wear mechanisms. It also discusses the potential applications of these modified titanium alloys in the aerospace industry (Wang, Jiang, & Liu, 2002). A study investigated the unlubricated friction and wear of NiTiHf alloy treated with gas and plasma nitriding. Pin-on-disk tests revealed friction coefficients from 0.7 to 1.6 for nitrided disks and wear factors of about 10^{-6} for NiTiHf and plasma-nitrided disks, compared to 10^{-4} for gas-nitrided disks. Plasma nitriding offered better wear resistance, while gas nitriding resulted in more pin wear. The results are relevant for designing aerospace components like gears and fasteners (Stanford, 2019). Overall, the reviewed studies collectively underscore the importance of material treatment and alloy selection in enhancing the performance and durability of components in the aerospace sector, suggesting a trend toward using advanced materials like NiTi for critical applications.

Figure 1. SMA application on Boeing's variable geometry chevron (Costanza & Tata, 2020).

Lasers were first used in scientific studies in 1960. Today, continuous or pulsed lasers with high or very low power density are available in wavelengths ranging from infrared to ultraviolet radiation. Laser use has spread to many areas, such as communication, medicine, chemistry, and the defense industry. Among laser material processing, welding, cutting, drilling, surface treatment, alloying, shocking, and ablation are the first applications that come to mind. Material processing with laser is carried out in three ways: with melting (welding, surface melting, etc.), without melting (shocking, bending, etc.), or by evaporation (ablation, cutting, drilling, etc.) (Bahar, 2024).

Friction and wear are inevitable in various engineering applications where surface interactions occur. Various studies have been conducted to investigate the effect of intentionally created surface textures on the tribological performance of the material in contact with the surfaces moving against each other (Holmberg & Mathews, 1994; Priest & Taylor, 2000; Zhang, Deng, Ding, Guo, & Sun, 2017). Laser surface texturing (LST) is used as an effective and widespread method to modify the interaction between surfaces to provide better lubrication and wear resistance to engineering materials (Gachot, Rosenkranz, Hsu, & Costa, 2017; He et al., 2018; Menezes & Kailas, 2006; Vilhena et al., 2009).

The first successful application of LST dates back to the 1940s when an "interrupted surface finish" was developed at the diesel engine piston ring-liner interface to prevent seizure under hot operating conditions (Martz, 1949). In the 1960s, Anno et al. (Anno, Walowit, & Allen, 1968) proposed their theory on micro-asperity lubrication by adding protrusions to improve tribological performance. In the late 1990s, Etsion et al. (Etsion, 2004; Etsion & Burstein, 1996; Faces, 1994) proposed that micro-dimples on the surface of mechanical seals could reduce friction and improve wear resistance. Recently, Rosenkranz et al. (Rosenkranz, Grützmacher, Gachot, & Costa, 2019) and Grützmacher et al. (Grützmacher, Profito, & Rosenkranz, 2019) have summarized the state of the art of LST applied to mechanical components.

Over the years, various surface texturing techniques have been developed, including LST (Ryk & Etsion, 2006), ion beam etching/milling (Marchetto et al., 2008), lithography (Pettersson & Jacobson, 2004), hot embossing (Li, Xu, Liu, Wang, & Liu, 2016), micro-milling (Chen, Liu, & Shen, 2018), electrochemical machining (Walker, Kamps, Lam, Mitchell-Smith, & Clare, 2017), and mechanical texturing (Greco, Raphaelson, Ehmann, Wang, & Lin, 2009). Among these methods, LST has attracted significant attention due to its unique advantages, such as fast speed, high efficiency, good controllability, environmentally friendly structure, and the ability to produce surface texture with high complexity and accuracy (Earl, Castrejón-Pita, Hilton, & O'Neill, 2016; Kennedy, Byrne, & Collins, 2004; Kurella & Dahotre, 2005; Singh & Harimkar, 2012). Due to these advantages, LST has been widely used in various applications to improve the tribological performance of engineering components with contact surfaces, such as mechanical seals (Etsion, 2000), thrust bearings (Brizmer, Kligerman, & Etsion, 2003), piston rings (Ryk, Kligerman, Etsion, & Shinkarenko, 2005), and magnetic storage devices (Baumgart, Krajnovich, Nguyen, & Tam, 1995). Moreover, it has been used to improve the tribological performance of various materials, from metals (Tripathi, Gyawali, Joshi, Amanov, & Wohn, 2017; Xu et al., 2017) to ceramics (Meng, Deng, Liu, Duan, & Zhang, 2018; Xing, Deng, Gao, Gao, & Wu, 2018) and polymers (Maruo & Fourkas, 2008; Mitov & Kumacheva, 1998).

In this study, circular dimple-shaped patterns were created on the NiTi SMA samples' surfaces using the LST method. The effects of the surface texture on the COF value and wear rate were investigated.

2. Materials and Methods

In this study, materials obtained by purchasing from cylindrical NiTi alloy (51% Ni-49% Ti) shape memory alloy were used, and the test sample dimensions were prepared as 25x5 mm. The prepared test sample surfaces were polished by sanding and cleaned with alcohol. The LST process was performed with a femtosecond laser with a beam size of 15 µm, a wavelength of 250 fs, a frequency of 400 kHz, an average power of 1.25 W, a scanning speed of 10 mm/s, as surface ablation. The laser process was performed under normal atmospheric conditions, and no protective environment was applied. Some preliminary wear tests were performed to determine the appropriate experimental parameters, and the wear test parameters given in Table 1 were determined. Wear tests were performed in a ball-on-disc device (Turkyus, Turkey) in reciprocating motion mode, in a dry environment, and at room temperature. Then, the wear volume loss and specific wear rate values were calculated using the wear track profiles obtained from the 3D profilometer images. In addition, the values of friction coefficient for the laser-treated and untreated samples were compared. The SEM images were examined to evaluate the wear mechanisms.

Table 1. Wear test parameters

Abrasive ball	Load (N)	Sliding speed (mm/s)	Test duration (min)
∅6 mm WC ball Hardness 19 GPa	1	8	30
	3		

3. Result and Discussion

3.1. Abrasion of untreated surfaces

When the worn surface images and EDS analysis of the untreated NiTi SMA sample are examined (Fig. 2), it is seen that the width of the indentation formed at the end of the dry sliding wear test performed for 30 min under 1N load is approximately 800 µm (Fig. 2a). The place where the contact pressure is the highest and therefore, the plastic deformation occurs most severely is the middle region of the indentation (Küçük, 2020, 2021). There is delamination formation and wear waste transfer due to severe plastic deformation in the specified area (Fig. 2b). Transferred and smeared wear waste is observed in Fig. 2c. Still, it is seen that no microcracks are formed. The main reason for this situation is that NiTi SMA (Ni51Ti49) is in the stable austenite phase (B2 phase) at room temperature, in addition to the low load effect. Because the temperature increase caused by friction in the contact region supports the completion of the austenite phase transformation, the microstructure is in the austenite phase. Thus, it is evaluated that the contact area gains high elastic recovery ability, residual elongation is suppressed (Strnadel, Ohashi, Ohtsuka, Ishihara, & Miyazaki, 1995), and fatigue crack formation is prevented. In the examination made after the experiments carried out using the same test parameters under 3N load, it was seen that the wear scar width increased and reached 900 µm. Severe plastic deformation, abrasion, and delamination traces were observed on the worn surface.

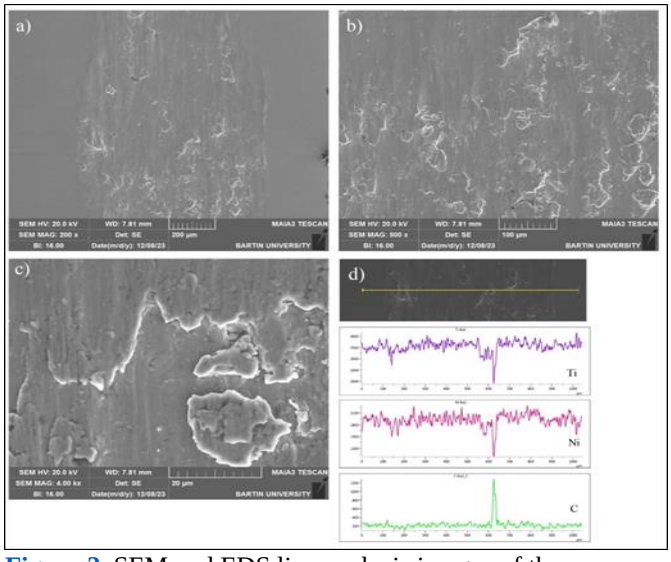

Figure 2. SEM and EDS line analysis images of the worn surface after the wear test of the NiTi SMA sample without LST application (load: 1N) a) 200x b) 500x c) 4kx d) EDS line analysis of the wear trace.

The 3D profilometer images of the worn surface of the samples under 1N and 3N loads are given in Fig. 3. As seen in Fig. 3a, the depth and width of the scar are approximately 7 µm and 600 µm, respectively, and abrasive wear is the dominant mechanism on the scar surface. In the worn surface image under 3N load (Fig.3b), it is understood that the depth and width of the scar are approximately 22 µm and 850 µm, respectively. The worn scar surface formed under 3N has a smoother contour, and rough abrasive wear marks are on the surface.

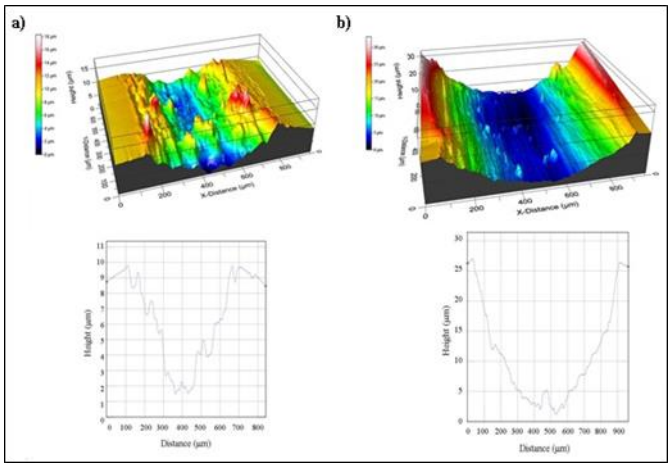

Figure 3. 3D profile images of the worn surface of the NiTi SMA sample without LST application a) 1N, b) 3N.

3.2. Wear of laser-applied surfaces

The optical microscope (OM) image taken after surface texturing is given in Fig. 4. The areal laser pattern density of the ablation region is 34%.

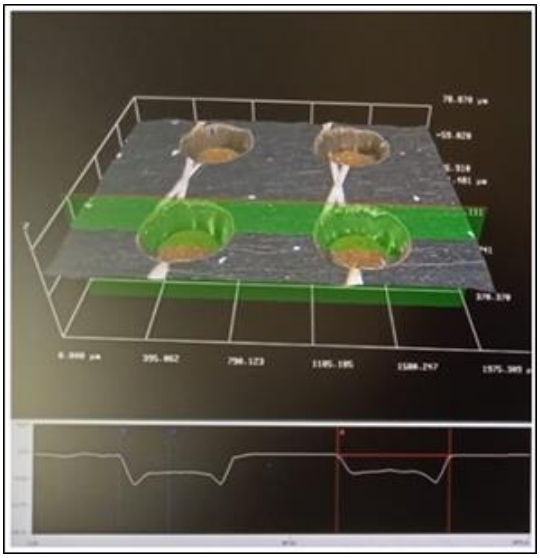

Figure 4. OM surface image of NiTi SMA after LST process.

When Fig. 4 is examined, it is seen that the ablation on the surface after the laser process is circular and 440 µm in diameter. The circular pit pattern has a conical structure that narrows inward and is approximately 42 µm deep. Fig. 5 shows the SEM images of the worn surface of the laser-ablated surface under 1N load.

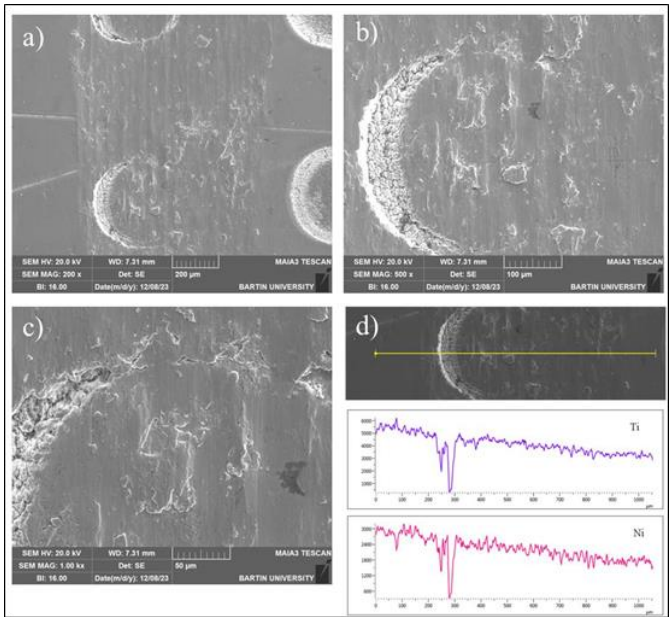

Figure 5. SEM and EDS line analysis images of the worn surface of the LST-applied NiTi SMA sample (load: 1N) a) 200x b) 500x c) 1kx d) EDS line analysis.

In addition to the plowing marks on the worn surface due to abrasion (Fig. 5b), delamination was also observed. In addition, the worn surface around the laser mark was smooth and even, and no microcracks or oxide layers were formed.

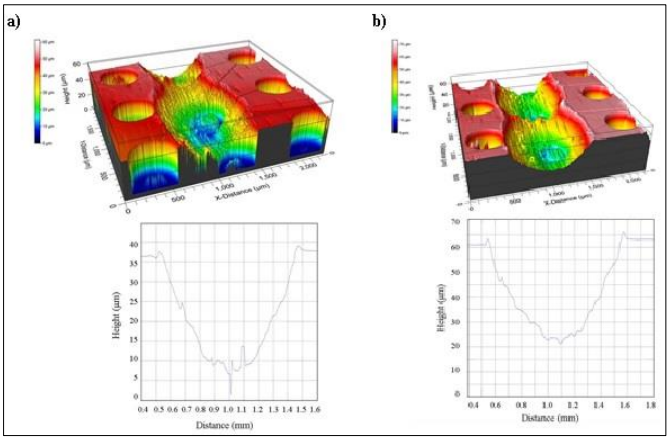

Figure 6. 3D profile images of the worn surface of the LST-applied NiTi SMA sample a) 1N, b) 3N.

Fig. 6 shows the worn surface images of the NiTi sample to which LST was applied under 1N and 3N loads. The depth of the scar formed under 1N load is 27 µm, while its width is 1000 µm (Fig. 6a). It is noteworthy that the laser pit trace on the surface was not erased after the wear test, and a scar formed around the laser trace in a widened and narrowed form. This situation is thought to occur due to fatigue crack formation and separation due to repeated loading at the trace edge. Fig. 6b shows the worn surface profile formed as a result of the wear of the surface after LST under 3N load. It is seen that the scar depth increased to approximately 40 µm under a 3N load, and its width remained almost the same as under a 1N load. It is understood from this that the amount of wear increased with increasing load.

Fig. 7 shows the worn surface SEM micrograph images of the sample to which the LST process was applied. It was observed that plastic deformation and abrasion wear occurred in the inner region and surroundings of the laser ablation scar. Wear particles were carried from the center of the scar to the edge and adhered to the surface (Fig. 7b). A smooth and even surface was formed due to plastic deformation around the laser ablation scar, and no microcracks were observed.

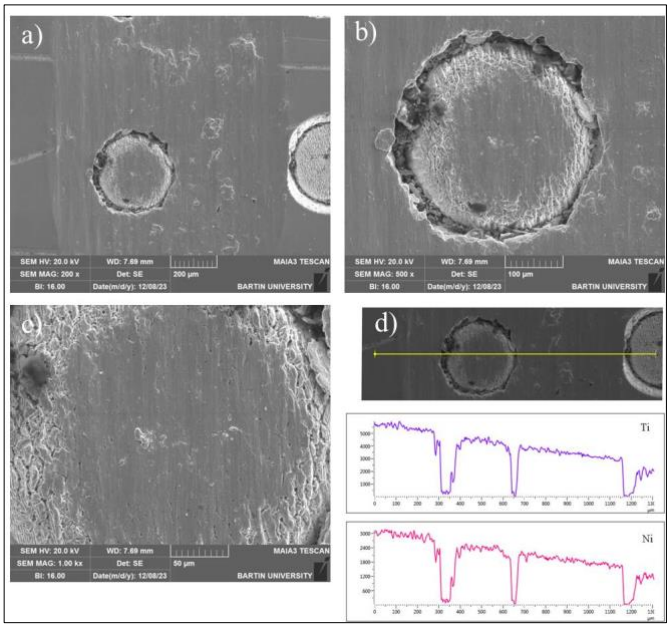

Figure 7. SEM and EDS images of the worn surface of the LST-applied NiTi SMA sample (load: 3N) a) 200x b) 500x c) 1kx d) EDS line analysis.

3.3. Changes in wear volume and friction coefficient before and after LST

The calculated wear volume loss, specific wear rate values, and friction coefficient graphs before and after LST are given in Fig. 8. As seen in Fig. 8a, the volume loss values in laser-applied samples are higher than those of untreated ones. It is thought that this situation is because the evacuation of the ablation area, which is quite broad compared to the width of the laser beam single pass, causes a long-term heat input and thus causes thermal softening in the heat-affected zone (HAZ) near the laser application region. This situation may be why microcracks do not form in LST samples. Thus, the tangential shear stress created by thermal softening and repeated friction causes more wear in the LST-applied sample. However, it is seen that the volume loss values increase with increasing load in all samples. According to Fig. 8b, the specific wear rate values decrease with increasing load in untreated and laser-ablation-applied samples; in other words, no directly proportional increase occurs. When the COF values recorded during wear are examined, it is seen that the COF values of the LST-applied samples decrease (Fig 8c). Similarly, it is understood that the COF values decrease with increasing load. The tangential friction force during sliding is decisive in determining the friction coefficient. The number of contacting surface roughnesses affects the tangential friction force. Since the number of contacts roughnesses decreases with laser ablation, the tangential friction force decreases, and the COF value decreases.

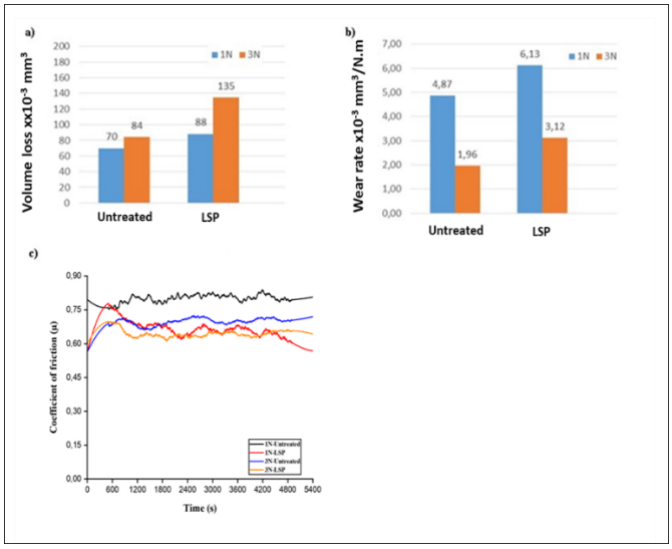

Figure 8. Graphical representation of NiTi samples before and after LST.

4. Conclusion

In this study, surface patterns in circular dimples with a diameter of 440 µm and a depth of approximately 40 µm were obtained by surface texturing (ablation) of NiTi SMA with a fiber laser. The results can be summarized as follows:

The pattern area density determined in surface texturing with the applied laser ablation process was 34%. Under 1N load, it caused a decrease of approximately 17% compared to the friction coefficient values of the samples without laser treatment. The reduction in the COF value under 3N load was calculated as approximately 14%.

When the wear volume loss values were examined, the volume loss values of the laser-applied samples were higher. The main reason for this is the thermal softening effect due to multiple laser passes due to the high ablation volume. It is estimated that the impact of LST on the wear behavior will also change with the reduction of the ablation surface area.

From the worn surface examinations, at low load (1N), a rough surface formed by wear track channels (grooving) and the plowing effect was formed on the untreated sample surface, while a smoother contoured wear track profile due to plastic deformation was obtained on the laser ablated sample surface.

Conflicts of Interest

The authors declare that there is no conflict of interest regarding the publication of this paper.

Acknowledgement

We would like to thank everyone at Lumos Laser for their contributions to the laser processes.

References

Abedini, M., Ghasemi, H., & Ahmadabadi, M. N. (2012). Effect of normal load and sliding distance on the wear behavior of NiTi alloy. Tribology Transactions, 55(5), 677-684.

Anno, J. N., Walowit, J., & Allen, C. (1968). Microasperity lubrication.

Bahar, H. (2024). Şekil hafızalı alaşımlara lazer ile yüzey modifikasyonunun aşınma davranışına etkisi. Yüksek Lisans Tezi, Bartın Üniversitesi, Lisansüstü Eğitim Enstitüsü.

Baumgart, P., Krajnovich, D., Nguyen, T., & Tam, A. (1995). A new laser texturing technique for high performance magnetic disk drives. IEEE Transactions on Magnetics, 31(6), 2946-2951.

Brizmer, V., Kligerman, Y., & Etsion, I. (2003). A laser surface textured parallel thrust bearing. Tribology Transactions, 46(3), 397-403.

Chen, L., Liu, Z., & Shen, Q. (2018). Enhancing tribological performance by anodizing micro-textured surfaces with nano-MoS2 coatings prepared on aluminum-silicon alloys. Tribology international, 122, 84-95.

Costanza, G., & Tata, M. E. (2020). Shape memory alloys for aerospace, recent developments, and new applications: A short review. Materials, 13(8), 1856.

DellaCorte, C., & Jefferson, M. (2015). 60NiTi intermetallic material evaluation for lightweight and corrosion resistant spherical sliding bearings for aerospace applications, report on NASA-Kamatics SAA3-1288. Paper presented at the Tribology Frontiers Conference.

Earl, C., Castrejón-Pita, J., Hilton, P., & O'Neill, W. (2016). The dynamics of laser surface modification. Journal of Manufacturing Processes, 21, 214-223.

Etsion, I. (2000). Improving tribological performance of mechanical seals by laser surface texturing. Paper presented at the Proceedings of The International Pump Users Symposium.

Etsion, I. (2004). Improving tribological performance of mechanical components by laser surface texturing. Tribology Letters, 17, 733-737.

Etsion, I., & Burstein, L. (1996). A model for mechanical seals with regular microsurface structure. Tribology Transactions, 39(3), 677-683.

Faces, L.-T. M. S. (1994). Analytical and Experimental Investigation of.

Gachot, C., Rosenkranz, A., Hsu, S., & Costa, H. (2017). A critical assessment of surface texturing for friction and wear improvement. Wear, 372, 21-41.

Greco, A., Raphaelson, S., Ehmann, K., Wang, Q. J., & Lin, C. (2009). Surface texturing of tribological interfaces using the vibromechanical texturing method.

Grützmacher, P. G., Profito, F. J., & Rosenkranz, A. (2019). Multi-scale surface texturing in tribology—Current knowledge and future perspectives. Lubricants, 7(11), 95.

He, Y., Zou, P., Zhu, Z., Zhu, W.-L., Yang, X., Cao, J., & Ehmann, K. F. (2018). Design and application of a flexure-based oscillation mechanism for surface texturing. Journal of Manufacturing Processes, 32, 298-306.

Holmberg, K., & Mathews, A. (1994). Coatings tribology: a concept, critical aspects and future directions. Thin Solid Films, 253(1-2), 173-178.

Jani, J. M., Leary, M., Subic, A., & Gibson, M. A. (2014). A review of shape memory alloy research, applications and opportunities. Materials & Design (1980-2015), 56, 1078-1113.

Kennedy, E., Byrne, G., & Collins, D. (2004). A review of the use of high power diode lasers in surface hardening. Journal of Materials Processing Technology, 155, 1855-1860.

Kurella, A., & Dahotre, N. B. (2005). Surface modification for bioimplants: the role of laser surface engineering. Journal of biomaterials applications, 20(1), 5-50.

Küçük, Y. (2020). Effect of counterbody on the dry sliding wear performance of plasma sprayed calcia-stabilized zirconia coating. International Journal of Refractory Metals and Hard Materials, 92, 105284.

Küçük, Y. (2021). Effect of counter body on wear behavior of plasma-sprayed TiO2-45Cr2O3 coating. Journal of Asian Ceramic Societies, 9(1), 237-252.

Li, N., Xu, E., Liu, Z., Wang, X., & Liu, L. (2016). Tuning apparent friction coefficient by controlled texturing bulk metallic glasses surfaces. Scientific Reports, 6(1), 39388.

Marchetto, D., Rota, A., Calabri, L., Gazzadi, G., Menozzi, C., & Valeri, S. (2008). AFM investigation of tribological properties of nano-patterned silicon surface. Wear, 265(5-6), 577-582.

Martz, L. (1949). Preliminary report of developments in interrupted surface finishes. Proceedings of the Institution of Mechanical Engineers, 161(1), 1-9.

Maruo, S., & Fourkas, J. T. (2008). Recent progress in multiphoton microfabrication. Laser & Photonics Reviews, 2(1-2), 100-111.

Menezes, P. L., & Kailas, S. V. (2006). Influence of surface texture on coefficient of friction and transfer layer formation during sliding of pure magnesium pin on 080 M40 (EN8) steel plate. Wear, 261(5-6), 578-591.

Meng, R., Deng, J., Liu, Y., Duan, R., & Zhang, G. (2018). Improving tribological performance of cemented carbides by combining laser surface texturing and WSC solid lubricant coating. International Journal of Refractory Metals and Hard Materials, 72, 163-171.

Mitov, Z., & Kumacheva, E. (1998). Convection-induced patterns in phase-separating polymeric fluids. Physical Review Letters, 81(16), 3427.

Otsuka, K., & Ren, X. (2005). Physical metallurgy of Ti–Ni-based shape memory alloys. Progress in Materials Science, 50(5), 511-678.

Pettersson, U., & Jacobson, S. (2004). Friction and wear properties of micro textured DLC coated surfaces in boundary lubricated sliding. Tribology Letters, 17(3), 553-559.

Priest, M., & Taylor, C. M. (2000). Automobile engine tribology—approaching the surface. Wear, 241(2), 193-203.

Rosenkranz, A., Grützmacher, P. G., Gachot, C., & Costa, H. L. (2019). Surface texturing in machine elements− a critical discussion for rolling and sliding contacts. Advanced engineering materials, 21(8), 1900194.

Ryk, G., & Etsion, I. (2006). Testing piston rings with partial laser surface texturing for friction reduction. Wear, 261(7-8), 792-796.

Ryk, G., Kligerman, Y., Etsion, I., & Shinkarenko, A. (2005). Experimental investigation of partial laser surface texturing for piston-ring friction reduction. Tribology Transactions, 48(4), 583-588.

Singh, A., & Harimkar, S. P. (2012). Laser surface engineering of magnesium alloys: a review. Jom, 64, 716-733.

Stanford, M. K. (2019). Dry sliding of nitrided NiTiHf. Tribology Transactions.

Strnadel, B., Ohashi, S., Ohtsuka, H., Ishihara, T., & Miyazaki, S. (1995). Cyclic stress-strain characteristics of Ti-Ni and Ti-Ni-Cu shape memory alloys. Materials Science and Engineering: A, 202(1-2), 148-156.

Sun, L., & Huang, W. (2009). Nature of the multistage transformation in shape memory alloys upon heating. Metal Science & Heat Treatment, 51.

Tripathi, K., Gyawali, G., Joshi, B., Amanov, A., & Wohn, S. (2017). Improved tribological behavior of grey cast Iron Under low and high viscous lubricants by laser surface texturing. Materials Performance and Characterization, 6(2), 24-41.

Vilhena, L., Sedlaček, M., Podgornik, B., Vižintin, J., Babnik, A., & Možina, J. (2009). Surface texturing by pulsed Nd: YAG laser. Tribology international, 42(10), 1496-1504.

Walker, J., Kamps, T., Lam, J., Mitchell-Smith, J., & Clare, A. T. (2017). Tribological behaviour of an electrochemical jet machined textured Al-Si automotive cylinder liner material. Wear, 376, 1611-1621.

Wang, H. M., Jiang, P., & Liu, Y. (2002). State of the art and prospects on laser surface modifications of titanium alloys for the aerospace industries. Lasers in Material Processing and Manufacturing, 4915, 167-172.

Xing, Y., Deng, J., Gao, P., Gao, J., & Wu, Z. (2018). Angle-dependent tribological properties of AlCrN coatings with microtextures induced by nanosecond laser under dry friction. Applied Physics A, 124, 1-11.

Xu, Y., Peng, Y., Dearn, K. D., You, T., Geng, J., & Hu, X. (2017). Fabrication and tribological characterization of laser textured boron cast iron surfaces. Surface and Coatings Technology, 313, 391-401.

Zhang, K., Deng, J., Ding, Z., Guo, X., & Sun, L. (2017). Improving dry machining performance of TiAlN hard-coated tools through combined technology of femtosecond laser-textures and WS2 soft-coatings. Journal of Manufacturing Processes, 30, 492-501.

Cite this article: Kucuk, Y., Altas, E., Gok, M.S., Bahar, H. (2024). Effect of Laser Surface Texturing Process on Dry Sliding Wear Behavior of NiTi Shape Memory Alloy Used in Airplane. Journal of Aviation, 8(3), 229-234.